

A Coupling Enhancement Algorithm for ZrO₂ Ceramic Bearing Ball Surface Defect Detection Based on Cartoon-texture Decomposition Model and Multi-Scale Filtering Method

(1.School of Mechanical and Electronic Engineering, Jingdezhen Ceramic University, Jingdezhen, People's Republic of China)

(2. Laboratory of Ceramic Material Processing Technology Engineering, Jiangxi 333403, PR China)

(3.National Engineering Research Center for Domestic &Building Ceramics, Jingdezhen, People's Republic of China)

Wei Wang^{#1,2}, Xin Zhang^{#1,2}, Jiaqi Yi^{1,3}, Xianqi Liao^{1,2}, Wenjie Li^{2,3}, Zhenhong Li^{*1,3}

Abstract: this study aimed to improve the surface defect detection accuracy of ZrO₂ ceramic bearing balls. Combined with the noise damage of the image samples, a surface defect detection method for ZrO₂ ceramic bearing balls based on cartoon-texture decomposition model was proposed. Building a ZrO₂ ceramic bearing ball surface defect detection system. The ZrO₂ ceramic bearing ball surface defect image was decomposed by using the Gaussian curvature model and the decomposed image layer was filtered by using Winner filter and wavelet value domain filter. Then they were fused into a clear and undamaged ZrO₂ ceramic bearing ball surface defect image and detected. The experimental results show that the image denoising method of ZrO₂ ceramic bearing ball surface defect based on cartoon-texture decomposition model can denoise while retaining the image details. The PSNR of image is 34.1 dB, the SSIM is 0.9476, the detection accuracy is 95.8%, and the detection speed of a single defect image is 191ms / img. This method can effectively improve the efficiency and accuracy of ZrO₂ ceramic bearing ball surface defect detection.

Key words: ZrO₂ ceramic bearing ball; Surface defect detection; Cartoon-texture decomposition; Gaussian curvature model

1 Introduction

ZrO₂ ceramic bearing ball has the advantages of high reliability, high hardness, strong endurance, non-conductive and non-magnetic [1-3]. It is widely used in aerospace, military, new energy and other advanced fields [4-7]. During the production, processing and transportation of ZrO₂ ceramic bearing ball, its surface is easy to form surface defects such as scratches, pits, snowflakes and cracks [8-9]. Those defects will reduce the lubrication ability and service life of the bearing ball. Therefore, in order to ensure the service performance of ZrO₂ ceramic bearing ball, its defects must be detected quickly and efficiently [10-14]. At present, manual testing generally has the problems of high cost and low efficiency, and the nondestructive testing method based on image processing has the advantages of low cost and high efficiency [15-18]. Using image processing technology, aiming at the problem that the defect image is sensitive to noise [19]. A surface defect detection method of ZrO₂ ceramic bearing ball based on cartoon-texture decomposition is proposed, so as to realize rapid and efficient nondestructive detection.

Cartoon-texture decomposition separates the fuzzy factor and approximate noise intensity factor in the image by minimizing the regularization coefficient. It can denoise and retain most of the details of the image, which has been widely concerned and studied by many experts and scholars. Wang et al. [20] proposed a medical image filtering method for fast variational cartoon-texture decomposition. Verified by experiments that this method can retain the basic details, and it is

Corresponding author: Xin Zhang. Email: JXLOCMPT_E_VIP@163.COM

School of Mechanical and Electronic Engineering, Jingdezhen Ceramic University, Jingdezhen 333403, People's Republic of China; Laboratory of Ceramic Material Processing Technology Engineering, Jiangxi 333403, People's Republic of China

#The authors Wei Wang and Xin Zhang contribute equally. They are co-lead authors

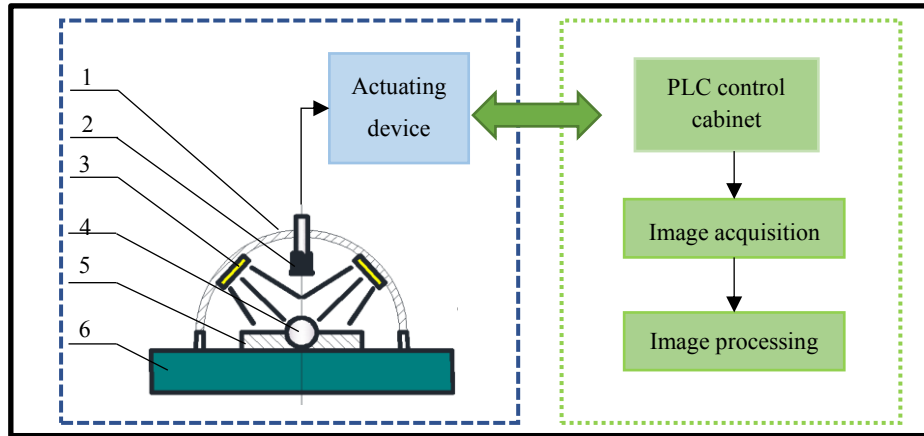
conducive to clinical detection and subsequent image segmentation. Chen et al. [21] designed a total variation denoising model based on Augmented Lagrangian algorithm to denoise the texture layer, and the simulation experiments show that this method can obtain high-quality images with high PSNR. Shang et al. [22] proposed a curvature guidance model that can promote image decomposition without divergence constraints, and introduced the level set region to filter the image. Experiments show that the model can protect edge details and repeated textures. Frédéric Sur [23] proposed a non-local dual domain method based on cartoon-texture decomposition. Established a zero-hypothesis texture power spectrum statistical model through experiments proved that this method can be applied to remote sensing image denoising regularly. At present, cartoon-texture decomposition is widely used in the field of image restoration, but this method is not perfect in the field of image denoising, and it is rarely applied to the field of ZrO₂ ceramic bearing ball.

Based on the previous algorithm research, in order to reduce the noise in the surface defect image of ZrO₂ ceramic bearing ball and retain the detailed features of the image at the same time. Solving the damage error caused by noise and filtering during surface defect detection. A surface defect detection method of ZrO₂ ceramic bearing ball based on cartoon-texture decomposition is proposed. By building a ZrO₂ ceramic bearing ball surface defect detection system, the ZrO₂ ceramic bearing ball surface defect image is decomposed by using Gaussian curvature model. Aiming to improve the detection accuracy and reduce the time-consuming. The decomposed image layer is filtered by Winner filter and wavelet value domain filter, and then fused into a clear and undamaged ZrO₂ ceramic bearing ball surface defect image.

2 ZrO₂ ceramic bearing ball surface defect detection system

2.1 Construction of ZrO₂ ceramic bearing ball surface defect detection experimental platform

For obtaining clear ZrO₂ ceramic bearing ball surface image, an experimental platform for ZrO₂ ceramic bearing ball surface defect detection as shown in Figure 1 is established. The experimental platform is divided into image acquisition module and image processing module. The image acquisition module is composed of CCD camera (Basler Med ace 2.3 MP 164 color, Basler vision technology (Beijing) Co., Ltd.), LED strip light source (c02-200x180, Dongguan wallop Automation Technology Co., Ltd.), light shield (c02-200x180, Dongguan wallop Automation Technology Co., Ltd.), PLC control cabinet (e2b-m18kn10-wz-b1, Omron Co., Ltd.), induction storage platform and experimental platform. The surface defect image is collected by the image acquisition module, stored by the image acquisition card and transmitted to the image processing module. First, installing the basic frame of the defect detection platform on the workbench, placing the ZrO₂ ceramic bearing ball sample on the stage, turning on the LED lamp and adjusting the brightness to an appropriate size to avoid edge blur due to the influence of light intensity on the quality of drawing. Then connect the CCD camera driving device to the high-performance computer, set the corresponding parameters, and adjust the magnification to an appropriate value until clear defects are seen. Finally, the captured ZrO₂ ceramic bearing ball surface defect image is stored in the image acquisition card, transmitted into the computer program and processed in the next step.



1-lens hood;2-CCD camera;3-LED strip source;4-ZrO₂ ceramic bearing ball;5-object table;6-work bench;

Fig. 1 Schematic diagram of testing platform for surface defects of ZrO₂ ceramic bearing ball

2.2 image acquisition and classification of surface defects

The surface defect classification and three-dimensional pixel diagram of zirconia ceramic bearing ball are shown in Figure 2. By analyzing the collected surface defect images of ZrO₂ ceramic bearing ball, it is found that there are four typical defect images in a large number of defects with different shapes. According to the shape characteristics, they are divided into pits, snowflakes, cracks and scratches. Pit defects are single point defects, snowflake defects are a cluster of irregular size, point defects are densely and disorderly arranged, crack defects are single strip defects, and scratch defects are densely arranged in a bundle of strip defects with different lengths. Through the analysis of the three-dimensional pixel diagram of each defect, it is found that there are defect information signals and noise signals in the diagram. These signals blend with each other. Some defect signals are obvious, but some defect signals are weak and exist in the noise. Therefore, the image noise signal and defect signal must be separated to reduce the error in defect detection.

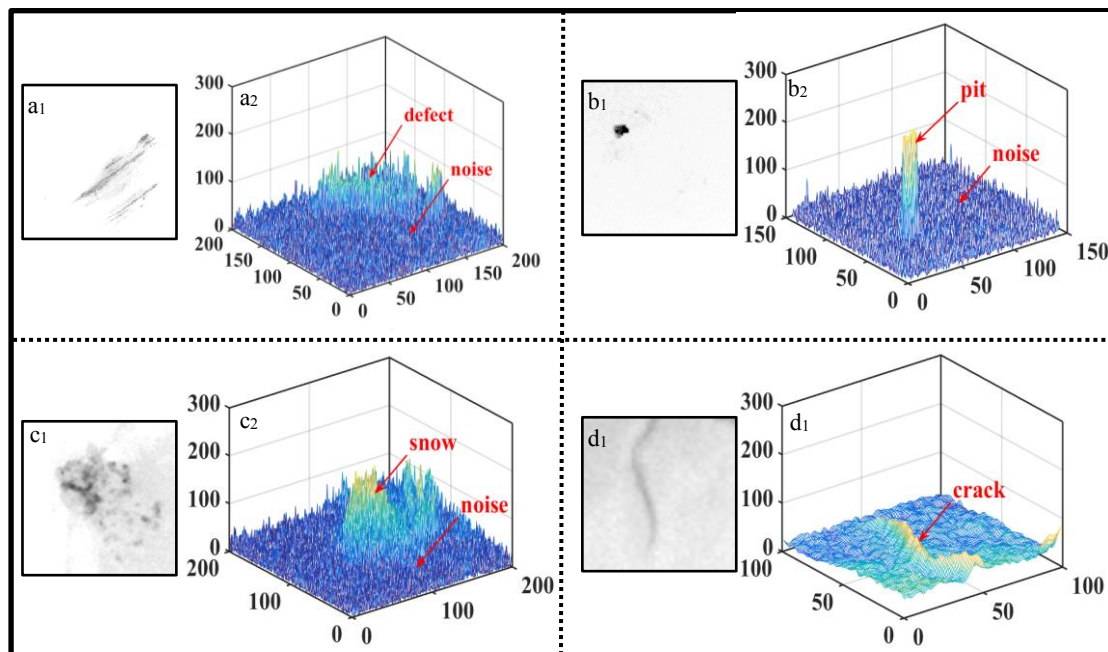


Fig. 2 classification and the 3D pixel map of surface defects of ZrO₂ ceramic bearing ball

Through the ZrO_2 ceramic bearing ball surface defect image detection platform, 60 ZrO_2 ceramic bearing ball surface defect images were collected, including 24 pit images, 9 snowflake defects, 14 crack defects and 13 scratch defects. The noise types of the collected defect images are random. In order to study the detection effect of the ZrO_2 ceramic bearing ball surface defect detection algorithm based on cartoon-texture decomposition on different noise images. As shown in Figure 3, the collected ZrO_2 ceramic bearing ball surface defect image data are subjected to Gaussian noise, pepper salt noise, mirror image processing, flip processing and color contrast enhancement. The surface defect detection of ZrO_2 ceramic bearing ball based on cartoon-texture decomposition model is carried out on the dataset image. From comparing the detection results to achieve the adaptability of ZrO_2 ceramic bearing ball surface defect detection algorithm.

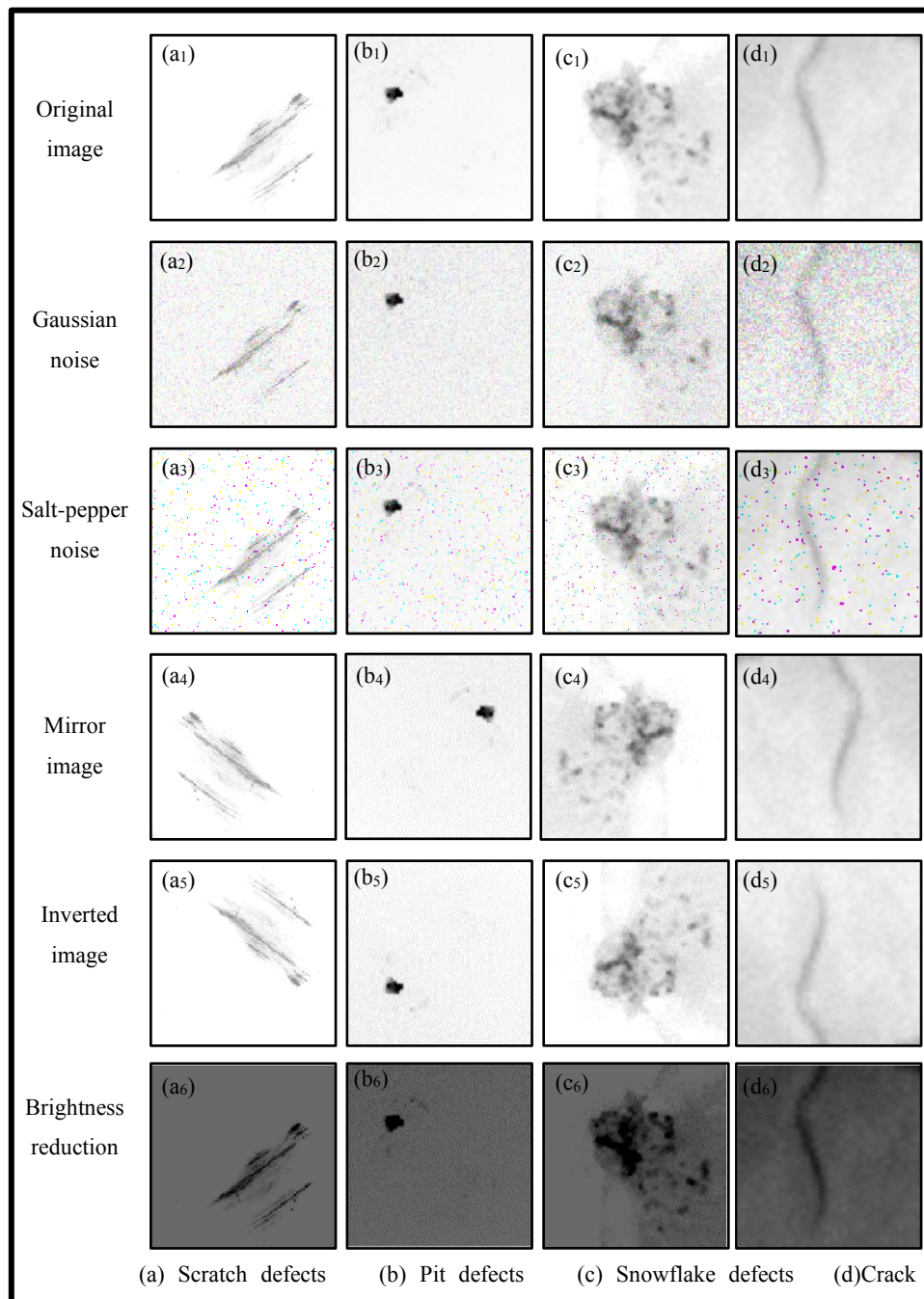


Fig. 3 Enhanced image data of ZrO_2 ceramic bearing ball's surface defects

2.3 Algorithm flow of ZrO₂ ceramic bearing ball surface defect detection

The algorithm flow of ZrO₂ ceramic bearing ball surface defect detection is shown in Figure 4. The defect detection process is mainly divided into four modules: image decomposition, image noise reduction, image fusion and defect detection. Firstly, the image is input to the image decomposition module, which is composed of cartoon-texture decomposition model based on Gaussian curvature model. The image is decomposed once to obtain the cartoon layer and the rest of the image. The cartoon layer is inversely colored and grayed and directly stored in the decomposition result, while the remaining part is composed of texture layer and deviation part. The deviation part is random and needs secondary decomposition. In order to minimize the deviation part, the remaining part is determined. There is a judge system that pure texture layer will be directly stored in the decomposition result and the deviation part will be regarded as the original image is decomposed again. Secondly, the decomposed result data is input into the image filtering module, the cartoon layer is subjected to winner filtering to obtain the image low-frequency subband, and the texture layer is subjected to wavelet hard value domain filtering to obtain the image high-frequency subband. Finally, the high and low frequency subbands are input into the image fusion part for wavelet inverse operation to obtain a clear ZrO₂ ceramic bearing ball surface defect image, which is input into the defect detection module for defect detection and classification.

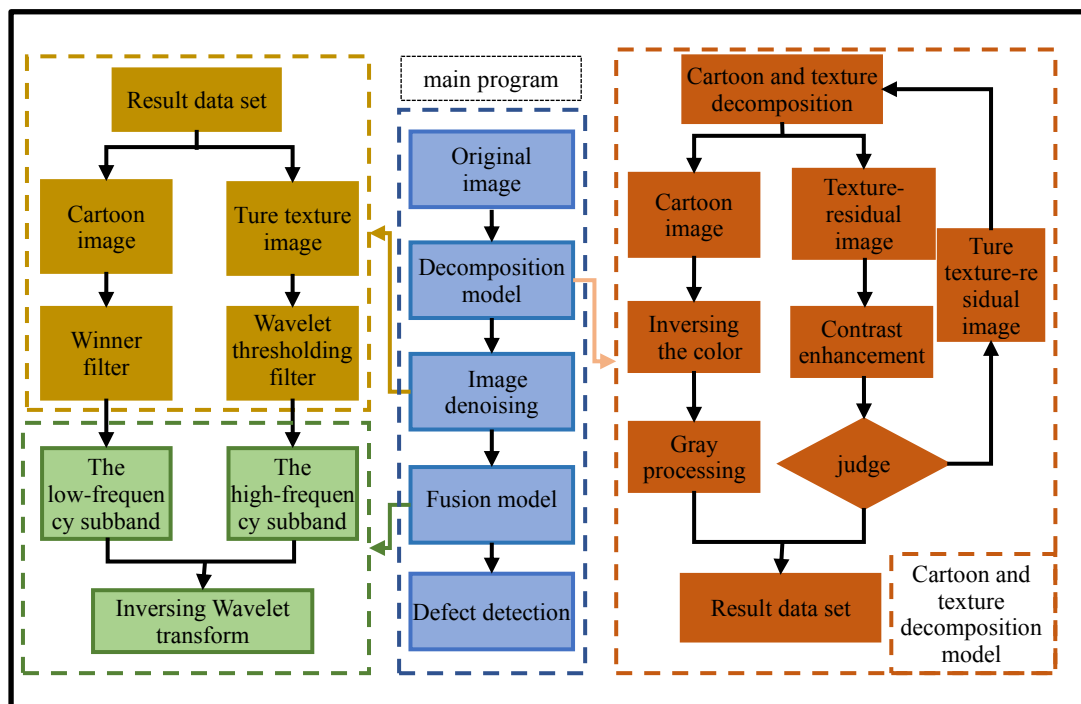


Fig. 4 flow chart of surface defect detection algorithm for ZrO₂ ceramic bearing ball

3. Surface defect detection process of ZrO₂ ceramic bearing ball

3.1 image decomposition of ZrO₂ ceramic surface defects

The defect detection of ZrO₂ ceramic bearing ball surface in industrial production mainly uses the characteristic that the reflection ability of the defective part to the light is quite different from that of the non-defective part [26]. The defects are detected and classified according to the gray value difference of each part in the image. Cartoon-texture decomposition decomposes the image containing defects and noise into strong noise texture image with significant edge information and smooth cartoon image.

Based on the Gaussian curvature variational model of the image, the original image is decomposed into cartoon part, texture part and deviation part, and the image decomposition model of ZrO₂ ceramic bearing ball surface defect is established. The mathematical expression is as follows:

$$O = \arg \min_{C,T} \int_{\Omega} (C \cdot T - O)^2 d\vec{i}d\vec{j} + M \int_{\Omega} |K(C)| d\vec{i} + N \int_{\Omega} |K(T)| d\vec{j} \quad (1)$$

Where: O is the original image of the surface defect of ZrO₂ ceramic bearing ball, which is required to be a piecewise curved surface; C is the cartoon part of the surface defect image of segmented smooth ZrO₂ ceramic bearing ball; T is the texture part of the surface defect image of ZrO₂ ceramic bearing ball, and it is the segmentation constant with significant image edges and details; M is the positive parameter of equilibrium C ; N is the positive parameter of equilibrium T .

$$\begin{cases} \vec{i} = (x,y) \in \Omega C \\ \vec{j} = (x,y) \in \Omega T \end{cases} \quad (2)$$

Where: \vec{i} and \vec{j} represent coordinate space; ΩC is the two-dimensional image fields of C . ΩT is the two-dimensional fields T .

$$\|C \cdot T - O\|_2^2 \quad (3)$$

Where: $|C \cdot T - O|$ represents the deviation part to ensure the consistency between $C \cdot T$ and O . At the same time, constraints need to be added to make the mean value of O less than or equal to the mean value of T ;

$$\begin{cases} \int_{\Omega} |K(C)| d\vec{i} = \int_{\Omega} K_1 K_2 d\vec{i} \\ \int_{\Omega} |K(T)| d\vec{j} = \int_{\Omega} K_1 K_2 d\vec{j} \end{cases} \quad (4)$$

$$\begin{cases} K(C) = \frac{C_{xx}C_{yy} - C_{xy}^2}{(1 + C_x^2 + C_y^2)^2} \\ K(T) = \frac{T_{xx}T_{yy} - T_{xy}^2}{(1 + T_x^2 + T_y^2)^2} \end{cases} \quad (5)$$

Where: K_1 and K_2 are the principal curvature of a point on the surface, $K(C)$ and $K(T)$ are definitions from the Gaussian curvature method; $K(C)$ and $K(T)$ are obtained by diffusion method using partial differential. C_{xx} , C_{yy} , C_{xy} , C_x and C_y are the partial differential of C ; T_{xx} , T_{yy} , T_{xy} , T_x and T_y are partial derivatives of T .

3.2 hierarchical filtering of surface defect image of ZrO₂ ceramic bearing ball

Image filtering based on the image decomposition of ZrO₂ ceramic bearing ball surface defects can make the defect detection achieve the purpose of more accurate detection. According to the

data distribution characteristics of cartoon layer, texture layer and deviation part, Winner filter is selected to filter the cartoon layer of the image, wavelet hard value domain filter is used to filter the texture layer, and wavelet soft value domain filter is selected for the deviation part.

(1) Winner filtering

Winner filter is a kind of least mean square filter. Its function is bidirectional. It can not only reduce the noise of noisy images, but also enhance degraded images. In fact, the image decomposition of the surface defect of ZrO₂ ceramic bearing ball is an over smooth image. The cartoon image is usually an over smooth degraded image or a non-degraded image containing noise, so it needs to be filtered.

When there is noise in the decomposed cartoon layer, the Winner filter expression is as follows:

$$\hat{F}(\mu, \nu) = \left[\frac{Q(\mu, \nu)S_{\eta}(\mu, \nu)}{S_{\eta}(\mu, \nu)|H(\mu, \nu)|^2 + S_f(\mu, \nu)} \right] G(\mu, \nu) \quad (6)$$

Where: $H(\mu, \nu)$ is the Fourier transform of the degenerate function; $Q(\mu, \nu)$ is complex conjugate of $H(\mu, \nu)$; $G(\mu, \nu)$ is the Fourier transform of the degraded image; $S_{\eta}(\mu, \nu)$ is the power spectrum of noise; $S_f(\mu, \nu)$ the power spectrum for degraded images.

When there is no noise in the cartoon layer: let $S_{\eta}(\mu, \nu)$ equal to zero, the original formula can be simplified to the following expression:

$$\hat{F}(\mu, \nu) = H(\mu, \nu)G(\mu, \nu) \quad (7)$$

At this time, Winner filter will inverse filter the degraded image, which can prevent the image from distortion due to excessive degradation.

(2) Wavelet range filtering

Wavelet range filtering uses the wavelet transform of the image signal to determine the effective signal and noise of the image by whether the signal is continuous in space, and suppresses the noise by setting the noise signal to zero. Because the image signal is continuous in space and the noise signal is discontinuous in space, the wavelet coefficient corresponding to the image signal is very large and the wavelet coefficient corresponding to the noise is very small after wavelet transform. Wavelet value domain filtering can be divided into wavelet hard value domain filtering and wavelet soft value domain filtering. Wavelet hard value domain filtering is suitable for texture part filtering because it combines the discontinuity of texture part defect data and the characteristics of partial deviation data obtained by insufficient decomposition; The deviation part of wavelet soft range filtering is weak, and most of the signals are in the field of noise signal, which is suitable for noise part filtering.

Firstly, the cartoon layer is filtered by wavelet hard range filtering. The wavelet hard range filtering suppresses the noise by setting the noise part of the small coefficient to zero. The corresponding coefficient distribution of the noise in the wavelet domain meets the Gaussian white noise distribution. Then, wavelet soft range filtering is used for the remaining part generated by insufficient decomposition. Different from wavelet hard range filtering, wavelet soft range filtering refines the coefficients greater than. The mathematical expressions of wavelet hard range filtering and wavelet soft range filtering are as follows:

$$\varpi_{\lambda_1} = \begin{cases} \mu & |\varphi| \geq 3\sigma \\ 0 & |\varphi| \leq 3\sigma \end{cases} \quad (8)$$

$$\varpi_{\lambda_2} = \begin{cases} [\text{sgn}(\varphi)](|\varphi| - 3\sigma) & \varphi \geq 3\sigma \\ 0 & |\varphi| < 3\sigma \\ \mu & \varphi \leq -3\sigma \end{cases} \quad (9)$$

Where: ϖ_{λ_1} is the signal filtered by wavelet hard value domain; ϖ_{λ_2} is the signal filtered by wavelet soft range; μ represents the original signal, and most of the noise is located in the interval $[-3\sigma, 3\sigma]$.

3.3 surface defect detection of ZrO₂ ceramic bearing ball

Combined with the surface defect characteristics of ZrO₂ ceramic bearing ball, the denoised image is thresholded. Taking the pit image as an example. Firstly, the pit defect image is grayed to obtain the change curve of image gray value. The boundary threshold between foreground and background is obtained by using the global gray value. So as to carry out threshold analysis. The image is corroded and re-expanded by morphological operation. And the image target is separated from the background threshold to obtain the rectangular area containing the foreground. The rectangular degree of the foreground area is analyzed to obtain the minimum rectangular value area containing the foreground and fill it. The rectangular area is opened to obtain a clearer target contour, and then each area is filled with color. The overlapping part of the color is regarded as the defect target, and the rest is the background part. The thresholding process of pit defects on the surface of ZrO₂ ceramic bearing ball is shown in Figure 5. The threshold analysis of the pit image on the surface of ZrO₂ ceramic bearing ball shows that the boundary threshold is 102, which can separate the foreground and background of the picture and obtain a clear defect image outline.

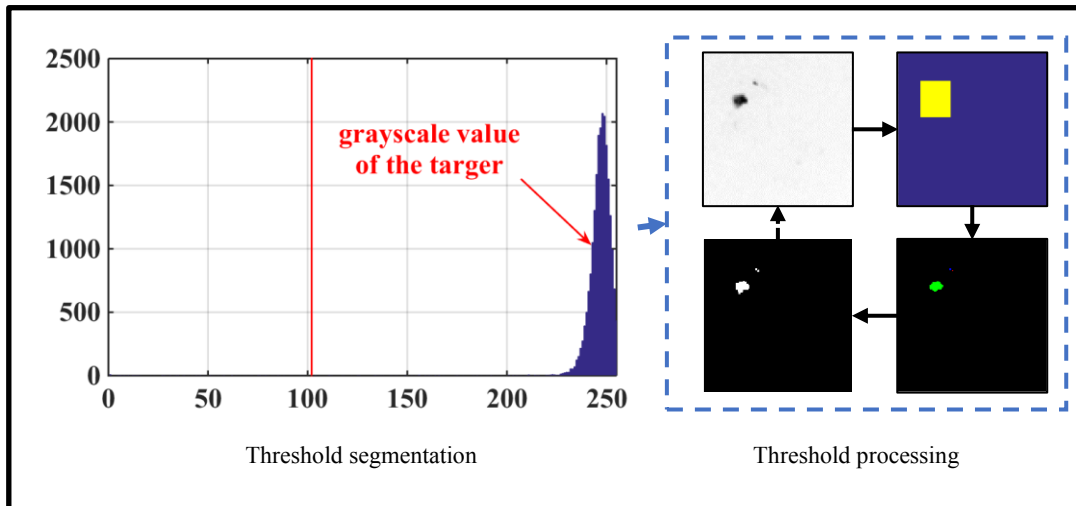


Fig. 5 The thresholding process of surface pit defect for ZrO₂ ceramic bearing ball

4 results and analysis

4.1 denoising effect analysis

The denoising process of ZrO₂ ceramic bearing surface defect image based on cartoon-texture decomposition model is shown in Figure 6. The left part is the ZrO₂ ceramic bearing ball surface

image processing process, the right part is the ZrO_2 surface defect image data analysis part. After inputting the image and analyzing the image signal, we can observe the defect information and noise information in the image. Decomposed the cartoon texture to obtain two gray and white images of the texture part and cartoon part of the image. By analyzing the gray and white image data, it was found that the texture part has obvious discontinuity, that was, the signal of the detail part and the noise part of the image were not fused, while the texture image has no noise signal and is relatively smooth. Then, the texture image was filtered by wavelet hard value domain, and the cartoon layer of the image was filtered by winner to obtain a clear cartoon image and a relatively soft texture image. Finally, the wavelet domain filter was used to fuse the image and analyze the final signal data of the image. The image noise was obviously suppressed and the defect information is clearer.

As a bi-directional image enhancement algorithm, Winner filter can skillfully make up for the problem of damaging the image when the cartoon texture is decomposed over smooth and the problem of noise residue when the image is not smooth enough. Aiming at the phenomenon of continuous texture detail information and discontinuous noise information in defect image, wavelet hard value domain filtering method can be used. When the deviation part cannot be set to zero in the experiment, the wavelet soft value domain filtering is used to obtain the deviation part, texture part and cartoon part. These three kinds of images are fused to obtain the denoised image with image details. The denoising algorithm of ZrO_2 ceramic bearing ball surface defect image based on cartoon-texture decomposition can enhance the defect image information and facilitate defect detection.

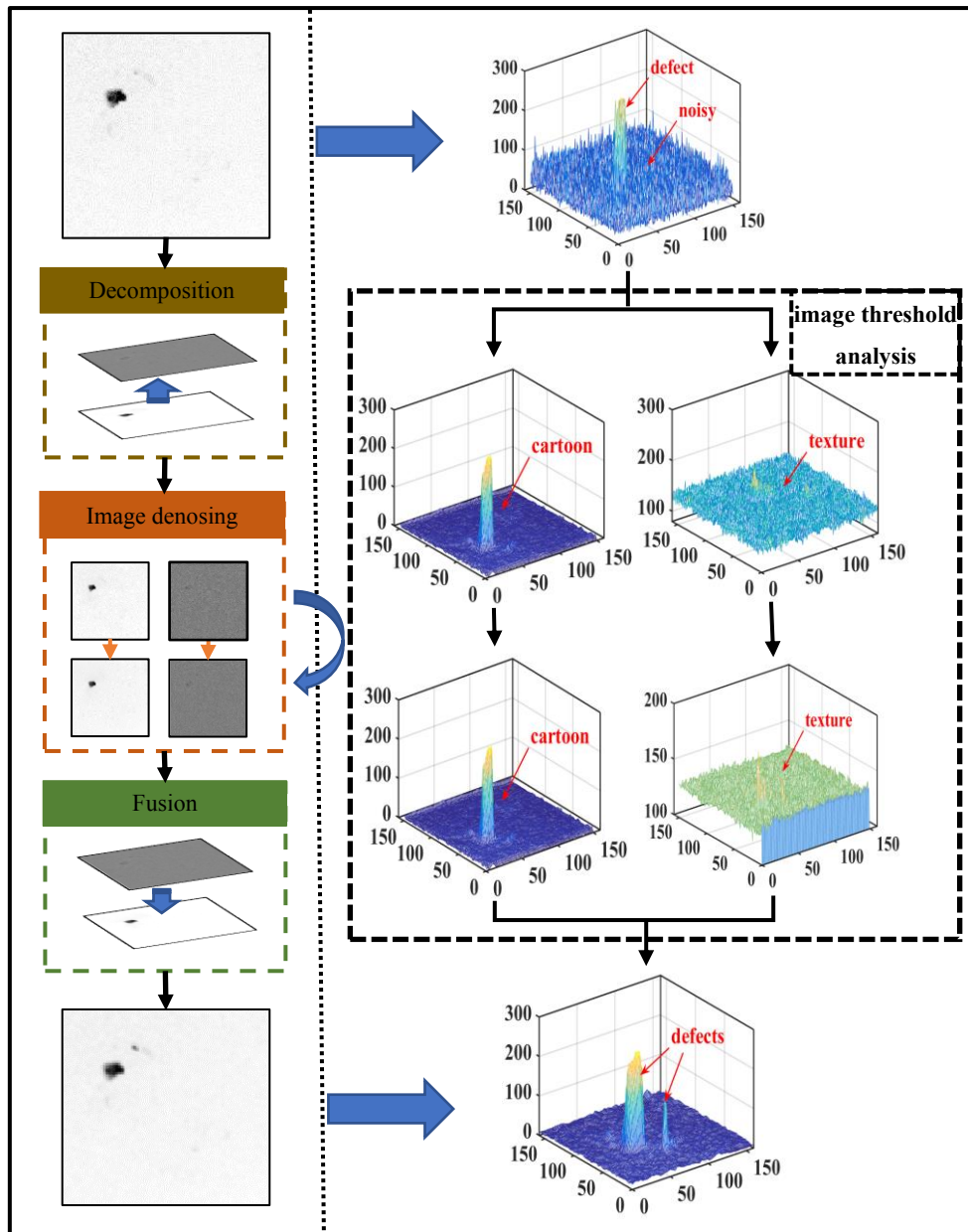


Fig. 6 Denoising process of ZrO₂ ceramic bearing surface defect image based on cartoon-texture decomposition model

4.2 Image quality analysis

The comparison of ZrO₂ ceramic bearing ball surface defect detection is shown in Figure 7. The denoised image and the original image are detected and the results are compared. The original image signal data of ZrO₂ ceramic bearing ball surface defect is thresholded to obtain the defect contour, and then the edge curve of pit defect image is obtained by edge detection; The defect contour is obtained by thresholding the defect signal data obtained by the ZrO₂ ceramic bearing ball surface defect image denoising algorithm, and then the edge curve of the ZrO₂ ceramic bearing ball surface pit image is obtained by edge detection. The experimental results show that the defect image denoised by ZrO₂ ceramic bearing ball surface defect algorithm can detect more minor defects, and the denoised image can suppress the noise and retain the details of image information at the same time.

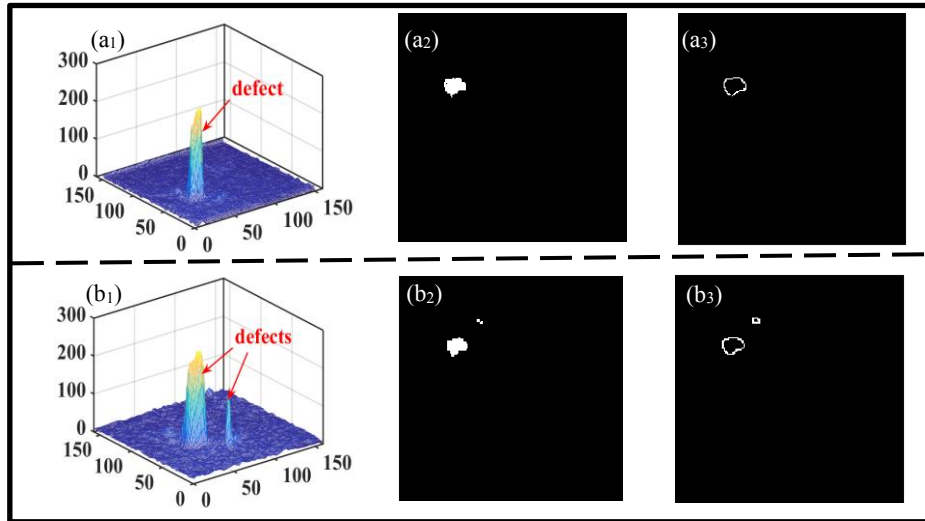


Fig. 7 Comparison of defect detection of ZrO₂ ceramic bearing ball's surface defects

For further analysis and clarify, the median filter, Winner filter, wavelet value domain filter and the filtering method in this paper are used to filter and analyze the scratch, pit, snowflake and crack defect images of ZrO₂ ceramic bearing ball respectively. The obtained results are compared with the data of the original image, and the average values of PSNR and SSIM are obtained respectively. The comparison of denoising effect of ZrO₂ bearing ball surface defect image is shown in Table 1. It can be seen from the table that the average PSNR of median filter, Winner filter, wavelet value domain filter and the algorithm in this paper are 22.6dB, 26.5dB, 25.6dB and 34.1dB respectively, and the average SSIM is 0.7815, 0.8213, 0.8066 and 0.9476 respectively. Compared the four denoising methods. The average PSNR and SSIM of the ZrO₂ ceramic bearing surface defect detection method based on the cartoon-texture decomposition model are better than the other three methods. It was proved not only ensures the denoising effect of the ZrO₂ ceramic bearing ball surface defect image, but also retains its detailed information.

Tab. 1 Comparison of denoising effect of ZrO₂ bearing ball surface defect image

Test image	median filtering		Winner filter		Wavelet range filtering		Filtering method in this paper	
	PSNR	SSIM	PSNR	SSIM	PSNR	SSIM	PSNR	SSIM
scratch	22.5	0.7546	28.6	0.8612	24.6	0.8854	34.6	0.9561
Pit	23.7	0.7825	27.4	0.8423	25.9	0.7942	35.7	0.9253
Snow	22.6	0.7933	25.3	0.7953	26.3	0.7823	33.4	0.9642
Crack	21.7	0.7956	24.8	0.7862	25.4	0.7643	32.7	0.9451
Mean	22.6	0.7815	26.5	0.8213	25.6	0.8066	34.1	0.9476

4.3 detection and analysis of surface defects of ZrO₂ ceramic bearing ball

In order to obtain a clearer surface defect image of ZrO₂ ceramic bearing ball and reduce the

probability of error in defect detection, it is necessary to denoise the surface defect image of ZrO_2 ceramic bearing ball. The four surface defects of scratch, pit, snowflake and crack are compared and analyzed by using local threshold algorithm, Otsu algorithm, OSTU threshold segmentation algorithm and this algorithm. The comparison of surface defect detection results of ZrO_2 ceramic bearing ball is shown in Figure 8. It can be seen from the figure that the detection results of the local threshold algorithm mostly omit the details of the image. The contour of the defect is not detected during the defect detection of the crack image. It is not suitable for the surface defect detection of ZrO_2 ceramic bearing ball. The surface defects of ZrO_2 ceramic bearing balls detected by Otsu algorithm have the loss of details and the blurring of defect contour. The defects detected by Otsu threshold segmentation algorithm do not omit details, but there is contour blur in crack image defect detection. The ZrO_2 ceramic bearing ball surface defect detection algorithm based on cartoon-texture decomposition can well detect the detailed contour of the defect image, which is not easy to produce edge blur and clearly display the defect area.

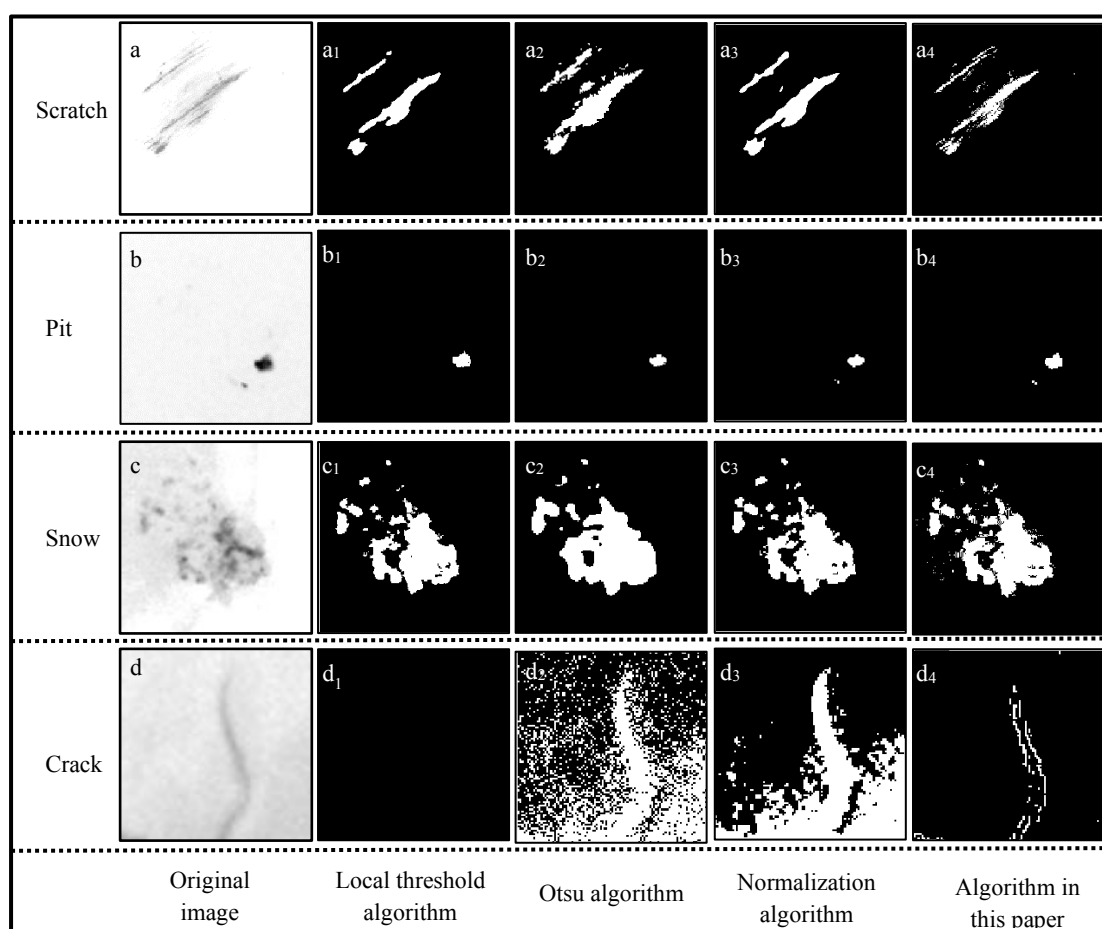


Fig8. Comparison of surface defects detection of ZrO_2 ceramic bearing ball

The classification effect of ZrO_2 ceramic bearing ball surface defects is compared, and its accuracy and time-consuming are calculated. The comparison of image classification results of ZrO_2 ceramic bearing ball surface defects is shown in Table 2. It can be seen from the table that the average accuracy of local threshold algorithm, Otsu algorithm, Normalization algorithm and this algorithm are 94.6%, 94.8%, 95.4% and 95.8% respectively, and the average time consumption is 143ms, 252ms, 253ms and 191ms respectively. Compared with the four algorithms, the average accuracy of ZrO_2 ceramic bearing surface defect detection method based

on cartoon-texture decomposition model is the highest; The average time of local threshold algorithm is the shortest, but its gray value difference between defect area and background area is small, and the image detection accuracy of subtle defects is not high. The proposed surface defect detection method of ZrO₂ ceramic bearing based on cartoon-texture decomposition model has good detection effect in terms of comprehensive accuracy and time-consuming. It can effectively improve the efficiency and accuracy of surface defect detection and classification of ZrO₂ ceramic bearing.

Tab. 2 Image classification report on surface defects of Si₃N₄ ceramic spheres

Test image	Algorithm	median filtering	Winner filter	Wavelet range filtering	Filtering method in this paper
Scratch	Accuracy	98.1%	94.3%	93.6%	97.8%
	Time(ms)	145	257	253	186
Pit	Accuracy	97.6%	100%	99.1%	100%
	Time(ms)	135	255	257	197
Snow	Accuracy	92.1%	91.3%	93.5%	93.1%
	Time(ms)	154	260	247	196
Crack	Accuracy	90.6%	93.7%	95.6%	92.4%
	Time(ms)	138	236	253	187
Mean	Accuracy	94.6%	94.8%	95.4%	95.8%
	Time(ms)	143	252	253	191

5 Conclusion

(1) due to improve the accuracy of ZrO₂ ceramic bearing ball surface defect detection. Combined with the noise damage of image samples. A ZrO₂ ceramic bearing ball surface defect detection method based on cartoon-texture decomposition model is proposed. This method can denoise while retaining the image details. The image PSNR is 34.1 dB, the SSIM is 0.9476, the detection accuracy is 95.8%, and the detection speed of a single defect image is 191ms / img, which effectively improves the efficiency and accuracy of ZrO₂ ceramic bearing ball surface defect detection.

(2) by building a ZrO₂ ceramic bearing ball surface defect detection system. The ZrO₂ ceramic bearing ball surface defect image is decomposed by using Gaussian curvature model. The decomposed image layer is filtered by Winner filter and wavelet value domain filter to fuse into a clear and undamaged ZrO₂ ceramic bearing ball surface defect image and detect it. This method has certain guiding significance for improving the detection accuracy of ZrO₂ ceramic bearing ball surface defects.

Disclosure statement

No potential conflict of interest is reported by the author(s).

Funding

This work is supported by the National Natural Science Foundation of China [grant number: 52065028 and grant number:51705224].

This research was supported by the National Natural Science Foundation of China

References

- [1] Sivaranjani Gali, Ravikumar K., B.V.S. Murthy, et al. Zirconia toughened mica glass ceramics for dental restorations. *Dental Materials*. 2018;34(3): 36-45.
- [2] Kyungmok Kim. Analysis of frictional behavior of electrodeposited coatings against spherical counterfaces. *Journal of Coatings Technology and Research*. 2015; 12: 603-608.
- [3] Rodaev VV, Zhigachev AO, Tyurin AI, et al. An Engineering Zirconia Ceramic Made of Baddeleyite. *Materials*. 2021; 14(16):4676.
- [4] Khang D. Tran (2002). Burn-through resistance of fibre / felt materials for aircraft fuselage insulation blankets. *Fire and Materials*.2002;26(1): 1–6.
- [5] Huaitao Shi, Xiaotian Bai, Ke Zhang, Yuhou Wu, et al. Effect of Thermal-Related Fit Clearance between Outer Ring and Pedestal on the Vibration of Full Ceramic Ball Bearing. *Shock and Vibration*. 2018;15.
- [6] Walter Harrer, Marco Deluca, Roger Morrell. Failure analysis of a ceramic ball race bearing made of Y-TZP zirconia. *Engineering Failure Analysis*. 2014;36: 262-268.
- [7] K. Thoma, L. Rohr, H. Rehmann, et al. Materials failure mechanisms of hybrid ball bearings with silicon nitride balls. *Tribology International*. 2004;37(6): 463-471.
- [8] Branger E, Grape S, Jansson P. Partial defect detection using the DCVD and a segmented Region-Of-Interest. *Journal of Instrumentation*.2020: 15(07); 7009–7009.
- [9] Priyank Patel and V N Patel. Experimental study on enhancement of defect detection and defect size estimation in deep groove ball bearing. *Materials Science and Engineering*. 2020; 810: 012039.
- [10] Xu J Q, Zuo Z L, Wu D H, et al. Bearing Defect Detection with Unsupervised Neural Networks. *Shock and Vibration*. 2021;11.
- [11] V.N. Patel, N. Tandon, R.K. Pandey. Defect detection in deep groove ball bearing in presence of external vibration using envelope analysis and Duffing oscillator. *Measurement*. 2012;45(5): 960-970.
- [12] Alves MH, Constantini G, Ianni A, et al. Fire performance of non-load-bearing double-stud light steel frame walls: Experimental tests, numerical simulation, and simplified method. *Fire and Materials*. 2021;1–24.
- [13] Yang X.; Qiao T.; Zhang H, et al. Research on image recognition and detection method of sapphire bubbles. *Journal of Instrumentation*. 2019: 14(12); P12013–12013.
- [14] Liu J, Xu Z D, Xu Y J, et al. An analytical method for dynamic analysis of a ball bearing with offset and bias local defects in the outer race. *Journal of Sound and Vibration*. 2019, 461: 114919.
- [15] Zeng Z, Liu B, Fu J. et al. Reference-Based Defect Detection Network. *IEEE Transactions on Image Processing*. 2021; 30: 6637- 6647.
- [16] Ian S. Osborne. Electrical detection of diamond defects. *Science*.2017;11:707-708.
- [17] Wang W B, Zhao Y C, Wang X L. Pulsar Signal Denosing Method Based On Laplace Distribution in No-subsampling Wavelet Packet Domain. *The Astronomical Journal*. 2016; 152:131.
- [18] Zhang F., Fan H., Liu P., et al. Image Denoising Using Hybrid Singular Value Thresholding Operators. *IEEE Access*. 2020; 8: 8157-8165.
- [19] N. Dahraoui, M. Boulakroune, D. Benatia. New Deconvolution Technique to Improve the Depth Resolution in Secondary Ion Mass Spectrometry. *Journal of Nano- and Electronic Physics*. 2019; 11(2): 02021.
- [20] Wang J, Han X, Huang F et al. Local total variation cartoon-texture decomposition medical image filtering. [J] *Chinese Journal of medical physics*, 2019; 36 (08): 918-923.
- [21] CHEN F H, MA J, DAI J. X-ray image restoration method based on cartoon-texture decomposition. [J]. *Video engineering*,2016; 40(7): 123-127.
- [22] Shang W, Xu J, Guo Y, Cartoon and Texture Image Decomposition Driven by Weighted Curvature, *IEEE Access*, 2021.1-9.
- [23] Frédéric Sur. A Non-Local Dual-Domain Approach to Cartoon and Texture Decomposition. *IEEE*

transactions on image processing.2021;8: 1882-1894.

- [24] Gan, Y.S., Liong, S.T., Zheng, D. et al. Detection and localization of defects on natural leather surfaces. [J] Ambient Intell Human Comput (2021).